View Online

Fabrication of monolithic 3D micro-systems†

Pakorn Preechaburana[ab] and Daniel Filippini*[a]

Received 24th August 2010, Accepted 14th October 2010
DOI: 10.1039/c0lc00331j

This article describes a method and platform for fast prototyping of monolithic 3D microstructures, capable of producing arbitrary positive, negative and suspended 3D geometries, as well as sealed spaces and aligned 3D geometries using standard photoresists and few fabrication steps. Here a microfabrication method employing a mask-less micro-projection lithography platform, which co-exists on a routine fluorescence microscope, has been refined to produce a variety of 3D microstructures with up to 5 μm spatial resolutions and 10 : 1 aspect ratios, as well as its integration within macroscopic areas of several millimetres with up to 30 μm spatial resolutions.

Downloaded by Library of Chinese Academy of Sciences on 29 November 2010
Published on 02 November 2010 on http://pubs.rsc.org | doi:10.1039/C0LC00331J

Introduction

The micro-fabrication of complex 3D structures is relevant to microelectromechanical systems (MEMS), micro-fluidic devices, miniaturized sensors, and optical devices,[1–4] which find applications in diverse scientific fields. However, fabrication methods are typically restricted to specialists and production level facilities.[1] In conventional photolithographic methods, the chrome masks used to define device layouts contribute significantly to the overall cost and specialization of manufacturing procedures,[5] as well as limit layout flexibility since a new mask is required for each modification.

In exploratory research scenarios, the ability to iterate a design quickly and economically is essential. Mask-less photolithography can accelerate the process and make the workflow more versatile. Micro-stereo lithography (μSL[5–8]) is one of such mask-less techniques, which offers the possibility of complex 3D micro-structuring by sequentially exposing layer by layer of the structure, using dedicated specialized equipment.[6] Other methods used to create 3D microstructures employ gray-scale microfluidic photomasks,[9] printed color masks,[10] binary gray-level physical masks[11] and multiphoton absorption polymerization.[12] Alternatively, microscope projection lithography systems (MPLS),[5,13] which use patterned illumination controlled by digital micromirror devices (DMD),[14–18] offer affordable, versatile and direct conversion of computer designs into polymer microstructures, although the complexity of the 3D structuring is more restricted, and typically dedicated to positive geometries of single layers[14] and PDMS replica[19] templates.

At some point, the structures must be assembled, in order to confine samples within controlled 3D environments where reactions and measurements can take place. This typically implies additional manufacturing steps involving alignment and sealing procedures.[20–22]

[a]*Optical Devices Laboratory, Division of Applied Physics, IFM—Linköping University, S58183 Linköping, Sweden. E-mail: danfi@ifm.liu.se; Tel: +46 13 281282*
[b]*Department of Physics, Faculty of Science and Technology, Thammasat University, 12120 Prathumthani, Thailand*

† Electronic supplementary information (ESI) available: Exposure calibration and interface focusing procedure. See DOI: 10.1039/c0lc00331j

Here we demonstrate a fabrication procedure implemented as a MPLS that overcomes most of these obstacles in a concise way. This system co-exists as an accessory light source on routine fluorescence microscopes, and is capable of sophisticated 3D micro-structuring including the ability to configure sealed channels, monolithic cavities, suspended structures and aligned surfaces with arbitrary topologies using standard photoresists, as well as supporting the integration of the microstructures within macroscopic service areas.

Materials and methods

Fabrication platform

A Zeiss Axiovert 40 CFL inverted routine microscope was used as a microfabrication platform. The standard light source in this instrument is a modular component (HBO50AC), which was removed and replaced by a 2500 ANSI lumens Optoma EP1690 projector equipped with digital micromirror device (DMD), capable of a 1280 × 1024 pixels spatial resolution, 8 bits per color channel intensity resolution and a contrast range of 2500 : 1.

The projector internal UV filter was removed and the projector was aligned with the microscope fluorescence illumination path. A prime lens (Nikkor 50mm *f*/1.8) was used at its maximum aperture to redirect the light within the fluorescence illumination path (Fig. 1).

A mirror placed at the beam splitter position in the microscope's filter cube deflects the illumination towards the objective's back aperture, which focuses the light on the specimen. The excitation and emission filter are removed from the filter cube used for this process and the specimens are microscope glass slides (Menzel-Glaser) spin coated on one side with photoresist. During the fabrication process the photoresist is directly exposed or exposed through the glass slide by simple flipping over the slide on the specimen traverser.

The illumination focal plane is selected, at the photoresist surface and at the photoresist-glass interface for different stages of the process, using the microscope focusing screw.

During the focusing process, the dichroic beam splitter (Zeiss FT510 in a SET15 filter cube for rhodamine) produces a reflected image in the microscope's eyepiece that enables manual focusing. To avoid the exposure of the photoresist during the focusing

View Online

Downloaded by Library of Chinese Academy of Sciences on 29 November 2010
Published on 02 November 2010 on http://pubs.rsc.org | doi:10.1039/C0LC00331J

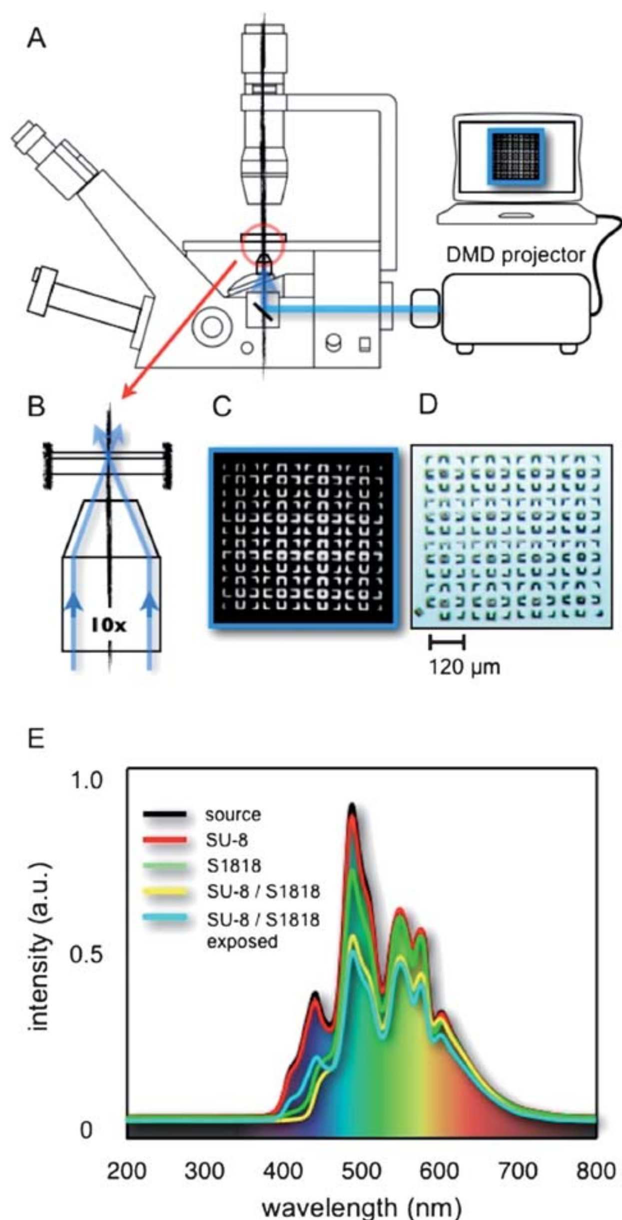

Fig. 1 Schematic of the fabrication instrumentation and principle. (A) Epi-fluorescence routine inverted microscope (Zeiss Axiovert 40 CFL) used as micro-fabrication platform operating with a patterned illumination provided by a DLP projector aligned with the fluorescence illumination path. (B) Magnification is commanded by objective selection. (C) An illuminating pattern with a minimum feature size of one pixel projected on the SU-8 sample can create microstructures (D) with a resolution of 5 µm and aspect ratios of 5 : 1 in the case of SU-8(10). (E) Spectral radiance of the light source measured on the microscope stage through a glass slide (black line), through 30 µm of SU-8 on glass (red line), 30 µm of SU8/S1818 on glass (yellow line) and the same material upon exposure (cyan line) and through 2 µm of S1818 on glass (green line). The perceived colors of the visible spectrum are indicated in the background.

process a green excitation filter is fitted to the filter cube (Zeiss BP 546/12). A common configuration of the microscope consists of a filter cube slider, which can accommodate three different cubes, which render focusing, and exposure as simple as switching to the next position in the cube slider.

For a 10× objective the working area compatible with tolerable distortions is limited to ~4 mm^2 and the achievable resolution is 5 µm (Fig. 1D). For the 2.5× objective the working area can be extended to ~50 mm^2, sufficient to fabricate structures in the mm range with ~30 µm resolutions.

Illuminating patterns

8 bits gray-level illuminating patterns are used to expose the photoresists. The patterns can be designed with various types of software (*e.g.* PowerPoint, Keynote, Open office Draw and Impress, *etc.*) and CAD. In this work the illuminating patterns were created with Matlab, displayed on a computer screen (Dell Latitude C640, Windows XP) connected to the projector.

Matlab can generate illuminating patterns with single pixel resolution, which are displayed without antialiasing. These conditions were deemed important to establish the resolution of the technique; however, the other alternatives are user friendlier and provide similar performance for features above ~15 µm in size.

The development process is not linear; consequently, developed structures do not correspond exactly to the target structures and illuminating patterns must be calibrated to compensate for nonlinearity.[27]

For this purpose, photoresist is exposed with a linearly varying intensity pattern and the height of developed structures is measured, yielding a sigmoid dose–response curve used to calibrate the exposure for each target profile (ESI1†).

Alignment procedures

For controlled negative spaces such as embedded channels, in the case of aligned microstructures or for cantilever structures, subsequent exposures must be aligned to configure the final geometry.

In the case of channels and cantilevers the walls and the supporting structure are first exposed from the glass side. The illuminating pattern is focused at the glass–photoresist interface using the microscope's focusing screw. The interface is indiscernible and focusing is achieved by calibrating the microscope focusing screw with the glass slide thickness and defocusing a properly focused illuminating pattern at the free glass surface, in the calibrated distance (ESI3†).

The exposed photoresist can be distinguished in phase contrast mode (Zeiss, 10×, 0.25, Ph1), the coordinates of the structure aligned using the grid of the eyepiece reticle in the microscope are positioned with the microscope sample traverser. During alignment a band-pass filter (Zeiss BP 546/12) is used to prevent exposure.

Once registered, the sample is flipped over in the microscope's sample holder and the illuminating pattern in the aligned position is now focused on the surface of the photoresist.

Switching to the next position in the filter cube's slider (cube without the excitation band-pass filter) the sample is exposed.

Binary masks

To fabricate the service structures and combined exposures such as in Fig. 2O, the fabrication platform is used to create binary Cr masks.

 This journal is © The Royal Society of Chemistry 2010

View Online

Downloaded by Library of Chinese Academy of Sciences on 29 November 2010
Published on 02 November 2010 on http://pubs.rsc.org | doi:10.1039/C0LC00331J

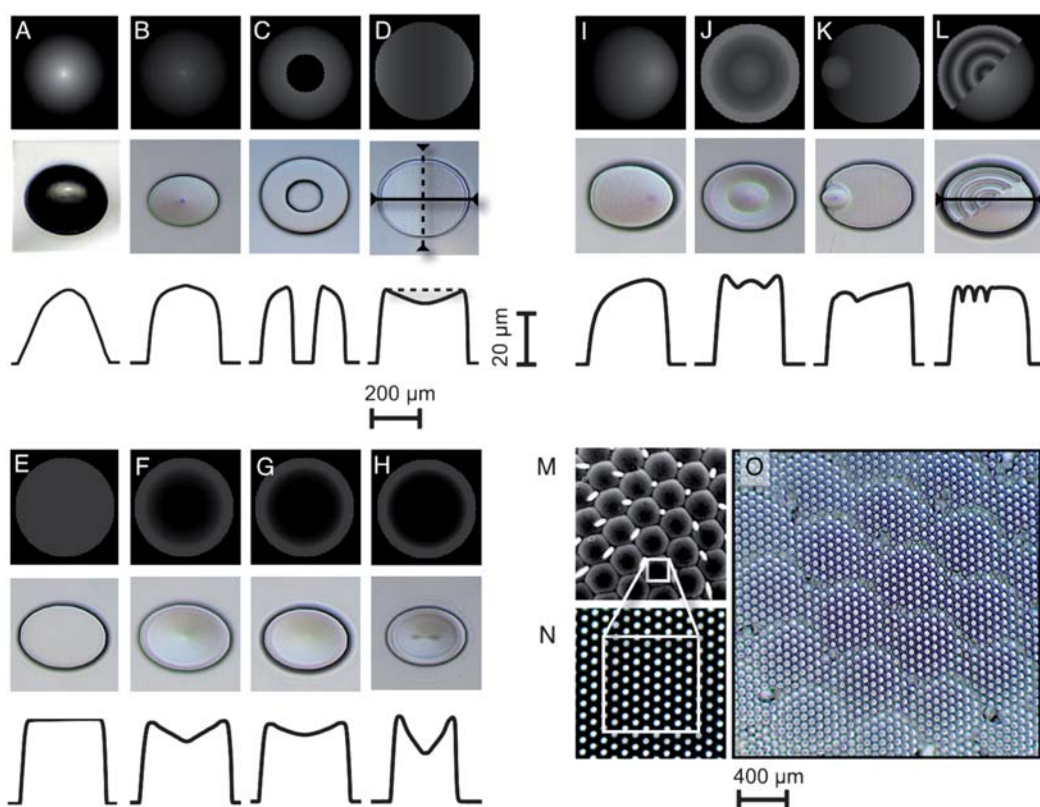

Fig. 2 Examples of single exposure 3D geometries. (A) Illumination pattern, microscope image and profilometry of a convex hemispherical surface. (B) Conic surface. (C) Conic surface with central hole. (D) Cylindrical concave surface. (E) Flat tip element. (F) Concave conic surface. (G) Concave spherical surface. (H) Concave aspherical surface. (I) Convex eccentric surface. (J) Combined concave–convex surface. (K) Combined convex small surface in an inclined plane. (L) Combined convex and rippled surface. (M) Picture of a Drosophila composed eye used as exposure pattern through a high contrast mask (N), which creates a projected pattern composed of high curvature elements of varied geometry.

For the service structures the 2.5× objective is used, whereas the 10× objective is used for the structures in Fig. 2O.

Cr thin films (150 nm) are deposited by thermal evaporation in a PVD platform operating at 10^{-6} Torr. Thickness was gravimetrically controlled using a quartz crystal microbalance (Inficon XTC).

Cr films spin coated with S1818 photoresist are exposed, using the fluorescence microscope, during 7 s through the 2.5× objective. Upon development of the S1818 photoresist, wet etching of Cr produces the mask.

In this work the Cr masks were used as disposable elements onto which the rest of the structures are fabricated. This mask transfer lithographic method[28] has the advantage of producing an intimate contact between the photoresist and the mask yielding well defined structures at the interface.

After exposure and development, the remaining Cr is removed by wet etching.

Characterization

A Dektak 6M stylus was used to measure the thickness and as well as capture 3D images of the microstructures.

The lateral size of the microstructures was measured with an optical microscope (Nikon, Optihot 66) fitted with a calibrated reticle.

The microscope images in this work were captured with a Cannon PowerShot A95, mounted to the camera channel of the Axiovert 40 fluorescence microscope.

Spectroscopic characterization of the light source at the microscope's sample stage was conducted with a fiber optic spectrophotometer (Ocean Optics USB2000).

Illuminating intensities were measured with a UVX-25 radiometer (UVP Inc.).

SU-8 and SU-8/S1818 processing

The substrates used in this work are microscope glass slides (Menzel-Glaser). Prior to photoresist coating, the slides were immersed in TL2 solution ($NH_3 : H_2O_2 : H_2O$ = 3 ml : 3 ml : 5 ml) at 85 °C for 5 min, followed by a DI water rinse, and baked to 200 °C on a hotplate for 5 min, to dehydrate the surface of the slides.

SU-8(10) and the mixture of SU-8(50) and S1818(SU-8(50)/S1818) were the photoresists used for the fabrication of 3D microstructures in this work.

SU-8 processing

SU-8(10) (MicroChem Corp.) was spin coated on slide using a SPIN150-NPP spin coater (SPS-Europe B.V.). After spin coating, the SU-8(10) is soft baked on a hotplate followed by

View Online

exposure on the fluorescence microscope. SU-8(10) is post-exposure baked on the same hotplate and subsequently developed. The processing protocol is outlined below.

Spin coating: SU-8(10) (MicroChem Corp.) photoresist (2 ml) is delivered to cover the whole slide, and spun at 500 rpm for 15 s at 1000 rpm s^{-1} acceleration followed by 30 s at 1000 rpm accelerating at 3000 rpm s^{-1}.

Soft baking: 65 °C for 3 min on hotplate, 85 °C for 7 min on hotplate.

Exposure: 135 mJ cm^{-2} (0.45 mW cm^{-2} for 5 min).

Post-exposure baking: 50 °C for 1 min on hotplate, 65 °C for 5 min on hotplate.

Development: immersion in developer (mr-dev 600, Microresist technology) for 5 min at room temperature, rinsed in isopropanol and dried in N_2 afterwards.

SU-8/S1818 processing

SU-8(50) (MicroChem Corp.) is mixed with 10% in volume of S1818 G2 (Rohm and Hass). The mixture has its absorption region at 400–450 nm, which can be supplied with the projector used in the platform.

SU-8(50)/S1818 is processed with the same equipments as the SU-8(10). The processing protocols are outlined below:

Spin coating: SU-8(10) (MicroChem Corp.) photoresist (2 ml) is delivered to cover the whole slide, and spun at 500 rpm for 15 s at 1000 rpm s^{-1} acceleration followed by 30 s at 1000 rpm accelerating at 3000 rpm s^{-1}.

Soft baking: 65 °C for 5 min on the hotplate, 85 °C for 25 min on the hotplate.

Exposure: 81 mJ cm^{-2} (0.45 mW cm^{-2} for 3 min) to produce the base of the structures, 27 mJ cm^{-2} (0.45 mW cm^{-2} for 1 min) to fabricate the suspended structures.

Post-exposure baking: 50 °C for 3 min on the hotplate, 65 °C for 15 min on the hotplate.

Development: immersion in developer (mr-dev 600, Microresist technology) for 2 h at room temperature, rinsed in isopropanol and subsequently dried in N_2.

Results and discussion

We fabricated 3D SU-8 and SU-8/S1818 microstructures of diverse complexity utilizing a routine inverted epi-fluorescence microscope (Carl Zeiss Axiovert 40 CFL) as a photolithographic platform, complemented with a conventional DLP projector (Optoma EP1690) as a light source. The projector lens was aligned with the microscope's fluorescence illumination optics through a prime lens (Nikon, Nikkor 50 mm). One of the microscope's filter cubes was fitted with a mirror to re-direct the illumination towards the target photoresist (Fig. 1A).

No permanent changes are made to any of the components, which can be readily reassembled in their original configurations. The fabrication platform described in this work coexists with routine use of the microscope and is implemented as an accessory. A design feature which renders this possible is the use of the epi-fluorescent channel for exposure, leaving the transmission path unaffected and fluorescence imaging operational for our routine fluorophores, since the spectral radiance of the projector source suffices to excite them.

The exposure pattern is generated in a computer and sent to the projector, either by coupling desktops or through a presentation program (*e.g.* Microsoft PowerPoint). The design of the exposure pattern can be directly created in the presentation software, in CAD applications or using designs reproduced from the literature, with the only precaution of keeping the smallest elements in the pattern compatible with projector resolution. Since modern digital micromirror device (DMD) projectors offer contrast ratios of 2500 : 1 or better, a single image pixel can properly expose the photoresists employed.

The illuminating pattern is focused on the photoresist through the objective lens (Fig. 1B). In the illustration the illumination is directed through the glass slide, but direct exposure from the SU-8 side is also possible, flipping over the sample. Both alternatives were used in this work to create 3D microstructures.

Using a 10× (0.25) A-plan objective lens and a projector spatial resolution of 1280 × 1024 pixels this platform can resolve features of 5 μm (Fig. 1C), which for 25 μm thick SU-8(10) photoresist allows 5 : 1 aspect ratios in an effective work area of 2 mm in diameter (Fig. 1D). Larger areas can be achieved exposing neighbor regions, which can easily be aligned, using the manual object traverser and an eyepiece reticle. Changing the objective to a 2.5×, the same platform can configure millimetre size structures (*e.g.* sample inlets) within an effective working area of 6 mm in diameter and ~30 μm resolution.

The source spectral radiance (black line) measured through a glass slide at the microscope stage using a fiber optics spectrometer (Ocean Optics USD 2000) is reproduced in Fig. 1E, with the visible colors of the spectrum displayed in the background. The radiance through glass, spin coated with SU-8 (30 μm thick), S1818 (2 μm) and SU-8/S1818 (30 μm), before and after exposure is indicated with red, green, yellow and cyan lines respectively. Strong absorbance in the blue part of the spectrum results from mixing SU-8 with S1818, rendering chromatic control of the exposure profile possible, across the thickness of the polymer, which is required to configure the negative geometries described in this work.

Beyond spatial resolution, one of the most versatile features of MPLS is the gray level (or color exposure[10]) capability that enables complete control of surface topologies in a snapshot exposure. All elements in the microstructure may be thus exposed simultaneously, with different intensities, which define the 3D topology. Fig. 2A–L summarize multiple examples which demonstrate these 3D capabilities: from plano-concave to plano-convex surfaces with arbitrary curvatures, to combined elements, all produced with a single exposure procedure. These are examples of the geometries achievable with the 8 bits gray level resolution possible in a single exposure of SU-8. As shown in Fig. 2A–H, the topology throughout the 30 μm thick SU-8 film is controlled in these examples. The bright field images of these geometries are shown together with their corresponding illuminating patterns and profilometry (Dektak 6M).

For the thickness, illuminating spectral radiance and exposure times considered above, the absorption profile of SU-8 is constant with thickness and it is indifferent to expose either from the glass or from the SU-8 side. For thicker films, shorter illumination bands and/or for modified SU-8, absorption profile and illuminating direction play an important role in the control of 3D geometry and enable to configure monolithic cavities and internal spaces.

Downloaded by Library of Chinese Academy of Sciences on 29 November 2010
Published on 02 November 2010 on http://pubs.rsc.org | doi:10.1039/C0LC00331J

 This journal is © The Royal Society of Chemistry 2010

Precisely controlled surface profiles are central to the fabrication of microoptical components, hence gray-scale lithography[10,23] is a convenient alternative to more expensive and demanding methods. The results summarized in Fig. 2 demonstrate that this approach is capable of SU-8 controlled 3D structuring compatible with such applications.

Although a single exposure is fast and simple, it does not exhaust the capabilities of this platform since the dynamic range can be extended by multiple exposures or by a combination of gray level single exposure with high contrast binary masks. The case illustrated in Fig. 2M–O provides an instance of such combination: a 150 nm thick chrome mask (Fig. 2N) configured with this platform, by wet etching of a chrome thin film on glass patterned with S1818 photoresist, was spin coated with SU-8, and exposed from the glass side allowing a high contrast exposure through the mask openings.

The use of a gray level illumination pattern with larger geometric features than those of the chrome mask (Fig. 2M) allows the configuration of complex compound geometries constituted by hundreds of pillar elements, each with its own distinctive topology (Fig. 2O). In this example the gray level pattern was from a picture of a Drosophila compound eye. The optical properties of this structure lie outside the scope of the present contribution, and its inclusion has been intended only to demonstrate the possibilities of the fabrication technique.

The purpose of this 3D microfabrication method includes not only arbitrary positive geometries, but also negative spaces of controlled geometry, such as vaulted cavities or channels, defined by monolithic microstructures properly sealed to the glass substrate. Such microstructures may be configured with only two exposure steps employing the most common photoresists (SU-8 and S1818).

The sample monolithic structure of Fig. 3A may be used to illustrate the fabrication method. The schematic represents the target geometry to be configured in photoresists and sealed to a glass substrate, which is represented atop of the structure. The sample geometry is meant to illustrate the ability of the fabrication method to confine separated spaces, to control the shape of internal spaces, and to align 3D microstructures in the vertical direction.

Fig. 3B–E summarizes the fabrication procedure. A glass slide spin coated with SU-8/S1818 is exposed on the microscope stage (Fig. 3B) from the glass side with the indicated illumination pattern. The projected pattern is focused at the photoresist–glass interface, which is indicated by a blue line in Fig. 3B. Precise focusing at the indiscernible photoresist–glass interface is achieved by calibrating the microscope focusing screw with the glass slide thickness and defocusing a properly focused illuminating pattern at the free glass surface in this distance (ESI3†).

The exposed polymer can be imaged by phase contrast, implemented in the same microscope and the structure registered using an ocular reticle and aligned for the next exposure step. Fig. 3C represents a cross-section schematics after exposure and the corresponding phase contrast image used for registration and alignment.

To complete the exposure, the sample is flipped over, in order to receive illumination from the polymer side as indicated in Fig. 3D. An 8 bits gray-scale pattern is used for illumination, which defines the concave and convex ceiling cavities required by the design, as well as the s-shaped trench embedded in the channel ceiling and the three through holes.

Once a target cross-section has been defined, the appropriate illumination pattern is established upon calibration (ESI1†). For instance, the fabrication of the concave ceiling in Fig. 3D–E requires an almost triangular illumination profile.

For this second and final exposure the illumination pattern is focused at the polymer surface (blue spectral line in Fig. 3G). Since the SU-8/S1818 mixture has a substantially larger absorbance than SU-8 in the blue region (Fig. 1E), the absorption profile in the z-direction may be controlled thus regulating the depth for proper photoresist exposure.

SU-8 is a negative photoresist, whereas S1818 is positive, which implies that during development, the SU-8 elements fixed by illumination correspond to those to be removed for S1818. However, the SU-8/S1818 mixture behaves as a negative photoresist with an increased absorption in the blue-green region of the spectrum (Fig. 1E). The combination of these materials also allows larger aspect ratios (10 : 1, ESI2†) than either single compound, and provides for easier removal, compared to SU-8, of the microstructure interior during development. In order to facilitate this process, openings and through holes must be provided in the layout design. Upon development, the unexposed polymer is removed and the finished 3D microstructure, sealed to the glass substrate is obtained (Fig. 3E).

The microscope image in Fig. 3E is taken from the glass side and illustrates the device fabricated with the design of Fig. 3A. The image is focused at the glass–photoresist interface, which shows a flat and well-sealed region. The inner details of the structure appear blurred due to limited depth of field, which is exceeded by the 300 μm deep microstructure (3D image in Fig. 3E).

The microstructure illustrated in Fig. 3E also includes convex SU-8 elements aligned in the z-direction, with a cross-section detailed in the inset. To create these aligned microstructures, the process begins with the fabrication of SU8 elements similar to those shown in Fig. 2. These microstructures are then coated with SU-8/S1818 and the process continues as detailed from Fig. 3B. Phase contrast imaging is used to align the SU-8 structures, with the first exposure pattern.

The tight sealing of the glass–polymer contact is demonstrated by the tests illustrated in Fig. 4. The microstructure described in Fig. 3 was filled with rhodamine and fluorescein solutions from two opposite directions. The solutions are isolated from each other, except at the contact between channels 1 and 2 (Fig. 4A), which mix within channel 1 (orange hue in channel 1 Fig. 4A).

The generation and control of multiphase flows are important in microfluidic structures to produce polymer particles, emulsions and foams,[2,24] whereas droplets also serve as compartments in microfluidic reactors.[25]

Fig. 4B and C illustrate alternate configurations, where controlled air–liquid interfaces are created within the microstructure. For a given fluid, air pockets ensue at predefined locations, with repeatable patterns (Fig. 4B), when the structure is filled with a solution. Different gas/liquid interfaces can be induced (Fig. 4C) by altering the geometry of the microstructure (*e.g.* changing the location of the roof holes).

An additional feature of interest is the ability to use the same platform to integrate the microstructures in a macroscopic scale compatible with direct sample delivery, for instance.

Downloaded by Library of Chinese Academy of Sciences on 29 November 2010
Published on 02 November 2010 on http://pubs.rsc.org | doi:10.1039/C0LC00331J

Published on 02 November 2010 on http://pubs.rsc.org | doi:10.1039/C0LC00331J
Downloaded by Library of Chinese Academy of Sciences on 29 November 2010

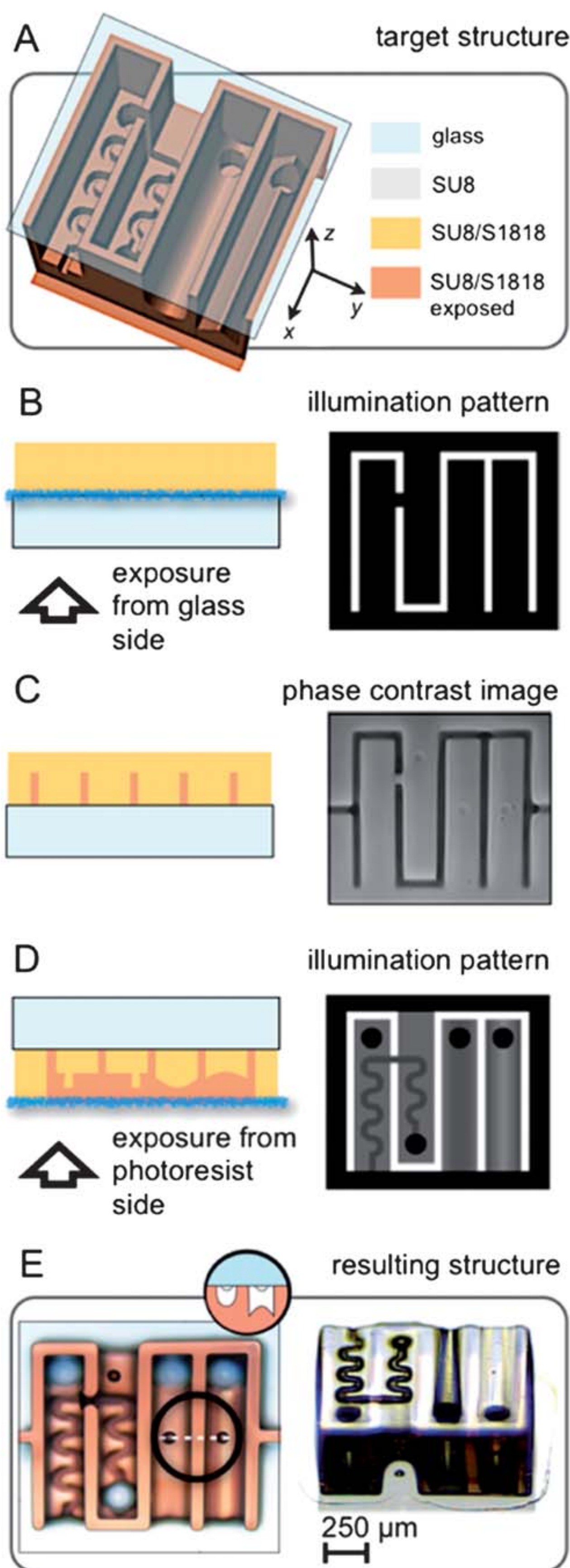

Fig. 3 Fabrication procedure of monolithic 3D aligned microstructures. (A) Target design of a 3D microstructure as seen from the glass side. The different colors correspond to the materials used to fabricate the microstructure. (B) SU8/S1818 spin coated on a regular glass slide is exposed from the glass side with the indicated illumination pattern, which defines the walls and polymer glass sealing of the microstructure. The illuminating pattern is focused at the glass–polymer interface, which is indicated by a blue line in B. (C) Schematic of the cross-section upon exposure and the phase contrast image of SU8/S1818 after exposure used to align the next exposure step. (D) Effect of exposure with the indicated illuminating pattern from the polymer side, which defines the geometry of the channel's cross-section. Illumination is focused on the polymer surface (blue line in D). (E) Microscope image of the finished structure observed from the glass side and 3D image from the topside. The inset indicates the cross-section of aligned geometries.

Switching microscope objectives makes it possible to change the scale of the structures; thus a 2.5× objective can be used to fabricate service structures of several millimetres with a resolution of about 30 μm.

Changing the objective lens reduces illumination and increases exposure times proportionally. Alternatively, the 2.5× exposure may be used to create a chrome mask, which is sufficient for the complexity of the service structures. Thus, the same platform was used to expose S1818 on a chromium thin film, which was subsequently etched to produce a mask. The S1818 exposure time is shorter than that required for SU-8 or SU-8/S1818 at this magnification, and the procedure still avoids more expensive mask fabrication methods.[26]

The macroscopic parts of the systems can be thus batch fabricated in SU-8 using the chromium mask by conventional photolithography, and the fabrication platform subsequently used to integrate the more complex microstructures. For this purpose, the SU-8 service structures are spin coated with SU-8/S1818 and transferred to the fabrication platform to complete the device.

The phase contrast image of an SU-8 microstructure spin coated with SU-8/S1818 (Fig. 4D) exhibits enough contrast (568/74 nm band-pass filtered illumination) to enable alignment while minimizing the exposure of SU-8/S1818. Upon exposure from the glass side at the registered position, the microstructure is connected to both SU-8 terminals. Fig. 4E is the phase contrast image of the exposed SU-8/S1818. To create the roof of the microstructure a final exposure is made from the polymer side.

In Fig. 4F the finished microstructure has been filled with a rhodamine solution, which circulates without leakages across the connections. The darker region in the center of Fig. 4F is due to a thinner roof in the region of the three connecting microchannels, used to regulate the flow. Fig. 4G–I are a time elapsed recording of the flow of rhodamine into fluorescein filled areas, which occur at a rate of ~25 μm s^{-1}. Structures without this restriction, such as the example in Fig. 4A, can be filled at rates larger than 300 μm s^{-1}.

In this work we have demonstrated 3D microstructures that can be integrated within ~50 mm^2 service areas. In fact, more than one 3D microstructure could be associated to each service area, since the required exposure times are less than 5 min for each 3D microstructure.

This journal is © The Royal Society of Chemistry 2010

View Online

Downloaded by Library of Chinese Academy of Sciences on 29 November 2010
Published on 02 November 2010 on http://pubs.rsc.org | doi:10.1039/C0LC00331J

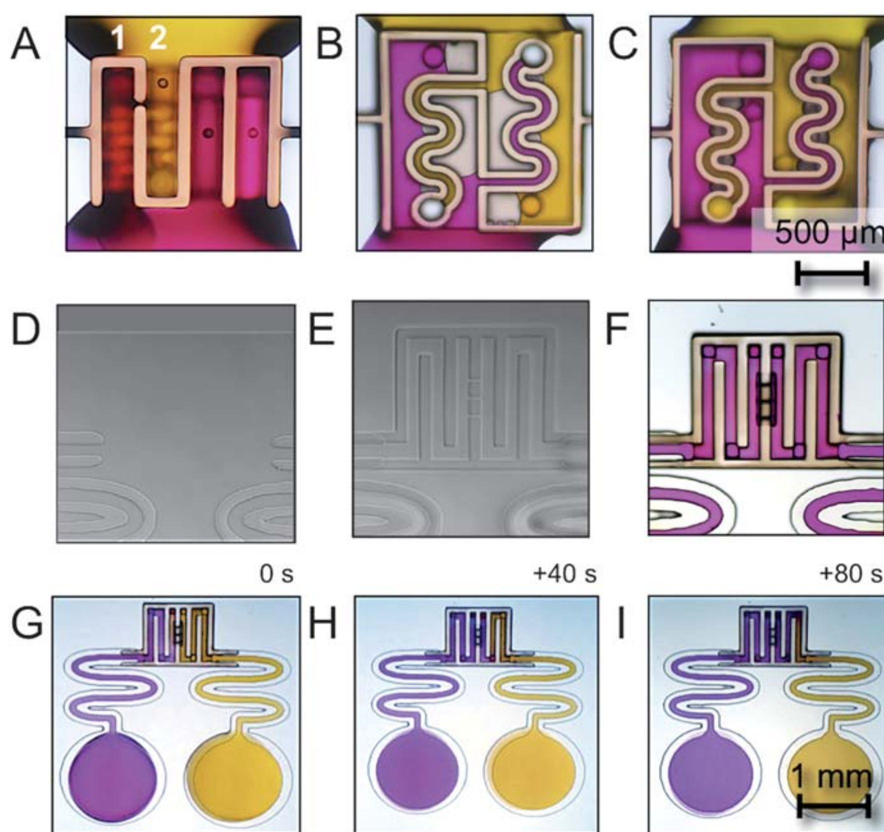

Fig. 4 (A) Microstructure of Fig. 3 filled with rhodamine and fluorescein solutions from opposite sides. Both solutions mix in channels 1. (B) S-Shaped channels and roof through holes with controlled gas/liquid interfaces. (C) Modified geometry producing a different configuration of air pockets. (D) Phase contrast image of service structure at the connection terminals. (E) Phase contrast image of the aligned microstructure upon exposure. (F) Microstructure circulated by a rhodamine solution across the service structure. (G) 2.5× magnification of the complete structure with rhodamine and fluorescein at the sample inlets. (H) Same as G but 40 s later. (I) Same as G but 80 s later.

Although the reproduction of this procedure is impractical for the larger service areas, due to the longer exposure times involved, it is still suitable with exposing the S1818 (only 7 s) used to pattern the wet etching of Cr masks. In fact, in this work we made multiple service areas in each glass slide by manually positioning the exposure pattern to different coordinates of the sample.

A programmable XY sample traverser could certainly be used not only to automatically reproduce these results but also to create cm long mask features by simultaneous displacement of the sample under the illuminating pattern. The same traverser could also provide systematic placing of specific 3D micro-structures in those extended layouts.

The ability to produce 3D negative geometries is relevant for fluidic devices and integrated optical elements among other uses. Default photolithographic methods produce constant rectangular cross-sections that restrict the possibility to control the 3D interfaces with a fluid. Hence, already configuring the channel height constitute a significant achievement, with the potential to control flow rate and shear stress in the fluid and to improve mixing and flow focusing.[9–11]

The example microstructures in this work illustrate geometric control beyond the channel height (like the S shaped channels in Fig. 3) and demonstrate the possibility to combine positive and negative geometries of arbitrary topology to define channel cross-sections.

A final capability, illustrated in Fig. 5, is the fabrication of cantilever structures of arbitrary cross-section. Fig. 5A shows an exposure pattern (illumination from the photoresist side) necessary to create the structures in Fig. 5B. A second exposure from the glass side (pattern not shown) is used to anchor the cantilever structures to the glass.

Using the same procedure previously described, it is possible to control the entire cross-section of the cantilever elements. For thick structures (>150 µm thick) the upper surface of the structure is flat, whereas if SU-8/S1818 deposits are sufficiently thin, the upper side of the polymer can also be structured as shown in Fig. 5B and in the detail of the spherical tip of the cantilever in

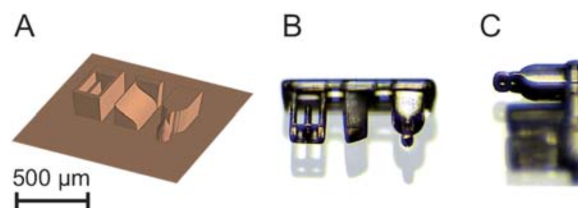

Fig. 5 (A) Exposure pattern for cantilever structures with controlled cross-sections. (B) 3D image of the resulting structures. (C) Detail of spherical suspended element.

View Online

Fig. 5C. Narrowing the connection to the anchor of the cantilever allows the fabrication of freestanding 3D elements.

Cantilevers of arbitrary topology embedded in a stream could serve as specialized obstructions for mixing purposes or for integrated sensing. Cantilever operating in static mode, bending due to selective binding of molecules,[29] is a possible alternative to explore with these fabrication capabilities and a type of solution compatible with integrated optical readout.[30]

These collective results demonstrate the ability to support a wide range of different components and subsystems, which may be integrated into larger systems, yet using methods and resources accessible to not only microfabrication specialists.

Conclusions

A microfabrication methodology capable of overcoming the obstacles and complexities of conventional approaches, whereas still delivering the sophistication required for practical microsystems, can be a valuable tool for microsystems development across most traditional disciplines.

The methodology and platform described here can provide substantial 3D microstructuring capabilities in a concise and affordable way, which may grant access to exploratory and customized microsystem design to regular users of microsystems.

Central to our solution is a refined methodology to use standard materials to deliver the full potential of a MPLS platform, demonstrated here through the fabrication of varied 3D microstructures such as monolithic cavities, sealed micro-channels, fully controlled surface topology of individual and multiply aligned surfaces and cantilever structures, as well as the ability to integrate such micro-structures within a macroscopic environment. This investigation shows that these capabilities can be met.

Acknowledgements

This work has been supported by a grant from the Carl Trygger Foundation of Sweden and a PhD scholarship from Thammasat University of Thailand for Mr Pakorn Preechaburana.

Notes and references

1 M. Madou, *Fundamentals of Microfabrication the Science of Miniaturization*, CRC, Boca Raton, Florida, 2002.
2 G. Whitesides, *Nature*, 2006, **442**, 368.
3 D. Psaltis, S. Quake and C. Yang, *Nature*, 2006, **442**, 381.
4 P. Yager, et al., *Nature*, 2006, **442**, 412.
5 J. Love, D. Wolfe, H. Jacobs and G. Whitesides, *Langmuir*, 2001, **17**, 6005.
6 C. Sun, N. Fang, D. Wu and X. Zhang, *Sens. Actuators, A*, 2005, **121**, 113.
7 K. Ikuta and K. Hirowatari, *IEEE Int. Conf. Micro Electro Mech. Syst., Tech. Dig., 6th*, 7–10 Feb 1993, **1**, 42.
8 X. Zhang, X. Jiang and C. Sun, *Sens. Actuators, A*, 1999, **77**, 149.
9 C. Chen, D. Hirdes and A. Folch, *Proc. Natl. Acad. Sci. U. S. A.*, 2003, **100**, 1488.
10 J. Taff, Y. Kashte, V. Spinella-Mamo and M. Paranjape, *J. Vac. Sci. Technol., A*, 2006, **24**, 742.
11 J. Atencia, S. Barnes, J. Douglas, M. Meacham and L. Locascio, *Lab Chip*, 2007, **7**, 1567.
12 G. Kumi, C. Yanez, K. Belfield and J. Fourkas, *Lab Chip*, 2010, **10**, 1057.
13 J. Behm, K. Lykke, M. Pellin and J. Hemminger, *Langmuir*, 1996, **12**, 2121.
14 K. Totsu, K. Fujishiro, S. Tanaka and M. Esashi, *Sens. Actuators, A*, 2006, **130–131**, 387.
15 T. Naiser, T. Mai, W. Michel and A. Ott, *Rev. Sci. Instrum.*, 2006, **77**, 063711-1.
16 J. Taff, Y. Kashte, V. Spinella-Mamo and M. Paranjape, *J. Vac. Sci. Technol., A*, 2006, **24**, 742.
17 J. Musgraves, B. Close and D. Tanenbaum, *Am. J. Phys.*, 2005, **73**, 980.
18 K. Totsu and M. Esashi, *J. Vac. Sci. Technol., B: Microelectron. Nanometer Struct.–Process., Meas., Phenom.*, 2005, **23**, 1487.
19 H. Wu, T. Odom, D. Chiu and G. Whitesides, *J. Am. Chem. Soc.*, 2003, **125**, 554.
20 Y. Song, C. Kumar and J. Hormes, *J. Micromech. Microeng.*, 2004, **14**, 932.
21 B. Chueh, D. Huh, C. Kyrtsos, T. Houssin, N. Futai and S. Takayama, *Anal. Chem.*, 2007, **79**, 3504.
22 S. Sawano, K. Naka, A. Werber, H. Zappe and S. Konishi, *IEEE Int. Conf. Micro Electro Mech. Syst., Tech. Dig., 21st*, 13–17 Jan 2008, 419.
23 C. Waits, A. Modafe and R. Ghodssi, *J. Micromech. Microeng.*, 2003, **13**, 170.
24 S. Xu, et al., *Angew. Chem.*, 2005, **117**, 734.
25 B. Yen, A. Günther, M. Schmidt, K. Jensen and M. Bawendi, *Angew. Chem.*, 2005, **117**, 5583.
26 S. Nicolas, E. Dufour-Gergam, A. Bosseboeuf, T. Bourouina, J. Gilles and J. Grandchamp, *J. Micromech. Microeng.*, 1998, **8**, 95.
27 C. Glasenapp and H. Zappe, *Opt. Eng. (Bellingham, WA, U. S.)*, 2008, **47**, 23002-1.
28 S. Macken and D. Filippini, *J. Micromech. Microeng.*, 2009, **19**, 85011–85016.
29 M. Nordstöm, et al., *Sensors*, 2008, **8**, 1595.
30 M. Nordstöm, D. Zauner, M. Calleja, J. Hübner and A. Boisen, *Appl. Phys. Lett.*, 2007, **91**, 103512.

Published on 02 November 2010 on http://pubs.rsc.org | doi:10.1039/C0LC00331J
Downloaded by Library of Chinese Academy of Sciences on 29 November 2010